FLUCOME 2009
10th International Conference on Fluid Control, Measurements, and Visualization
August 17–21, 2009, Moscow, Russia

ACTIVE CONTROL OF TURBULENT BOUNDARY LAYER USING AN ARRAY OF PIEZO-CERAMIC ACTUATORS

H L Bai and Y Zhou[#]

ABSTRACT

This paper presents preliminary results from an experimental exploration on drag reduction in a turbulent boundary layer using an array of piezo-ceramic actuators. The actuator array consisting of 16 actuators can generate wall-normal oscillations and, given a phase shift between two adjacent actuators, a spanwise travelling wave. A sinusoidal waveform with four different amplitudes was investigated while oscillating in a wide range of frequencies. The preliminary results showed that about 5% reduction in drag could be obtained based on the measurement of a hot-film flush-mounted on the wall. A drag increase up to 20% was also observed when the actuator array worked in large amplitudes and high oscillation frequencies. The possible mechanism of drag reduction behind this control technique was discussed. Investigations are on-going to use different control strategies such as different actuation signals, spanwise travelling wavelengths and speeds, etc. in order to achieve better results in terms of drag reduction.

Keywords: Active Control, Drag Reduction

1. INTRODUCTION

Active control of a fully developed turbulent boundary layer for drag reduction has recently attracted a great deal of attention. It has been demonstrated numerically and experimentally that the high wall shear stress is associated with the quasi-streamwise vortices (QSV), in particular the sweep events in the near-wall region, and inhibiting or annihilating these QSV can mitigate the turbulence production and reduce the skin friction (e.g. Kravchenko et al. 1993, Choi et al. 1994). Utilizing oscillatory spanwise cross-flow or wall motion, Jung et al. (1992) found that up to 40% drag reduction could be obtained in direct numerical simulation (DNS) when the oscillation period was $T^+ = 100$, where superscript "+" denotes normalization by wall variables. Choi et al. (1998) observed experimentally a reduction in skin friction downstream of an oscillating wall by as much as 45% and suggested that the spanwise speed, which was linked to both the oscillation amplitude and period, of the oscillating wall might be a crucial parameter in such an active control strategy. Although spanwise wall oscillation may achieve a significant drag reduction, its efficiency is low due to large energy consumption by the auxiliary mechanical motion (Quadrio & Ricco 2004). Based on their DNS data, Du & Karniadakis (2000) showed that a transverse wave induced by a spatial force travelling in the viscous sublayer could suppress dramatically the coherent structures in the near-wall region, resulting in a drag reduction exceeding 50%. The effect of

[#] Corresponding author: Department of Mechanical Engineering, The Hong Kong Polytechnic University, e-mail: mmyzhou@polyu.edu.hk

non-ideal waveforms, which might be practical in implementation, was also investigated in the simulation, showing that more than 20% drag reduction could be obtained (Du et al. 2002). Their preliminary experiment with Lorentz actuators produced results consistent with the DNS data. Nevertheless, this technique has yet to be demonstrated experimentally (Karniadakis & Choi 2003). Segawa et al. (2002) deployed an actuator array with 8 elements to disturb the near-wall structures. The actuator array aligned spanwise could realize three different modes, viz. the wavy mode, the alternating mode and the gathering mode. The perturbed flow structures under these modes were investigated using Particle Image Velocimetry (PIV), but no drag reduction was reported. The present work aims to investigate experimentally the drag reduction in a turbulent boundary layer using an actuator array. An array of 16 piezo-ceramic actuators, flush mounted with the wall surface and aligned in the spanwise, was used to generate the wall-normal oscillation and a transverse travelling wave given a phase shift between two adjacent actuators. Three distinct waveforms with four different amplitudes were tested while oscillating in a wide range of frequencies.

2. EXPERIMENTAL DETAILS

Experiments were conducted in a closed-circuit wind tunnel which has a 2.4-m-long test section of 0.6 m × 0.6 m. The boundary layer was produced by a 2.2-m-long Perspex flat plate, horizontally placed in the test section of the tunnel. The plate is 9 mm thick and has the same width of the tunnel. The distance between the surface of the plate and the ceiling of the test section is 450 mm. With the leading edge rounded to be an elliptic profile, the plate was slightly inclined to ensure a nearly zero-pressure gradient along the test section. A 200-mm-long end-flap plate, inclined in 10 degrees, was used to adjust the front stagnation line so as to avoid flow separation in the leading edge. At the location of 100 mm downstream from the leading edge, two spanwise-aligned arrays of M4 screws were used to trip the boundary layer. In each array a total of 59 screws, 5 mm high for each, were inversely stood with the spacing of 10 mm in the spanwise direction. The two arrays of screws were separated by 15 mm in the streamwise direction and were offset 10 mm in between in the spanwise direction. The oncoming velocity of the free stream is U_o = 4.0 m/s, monitored at exit of the contraction section by a Pitot tube, which was connected to a Furness micro-manometer (FC0510). The actuation location is L = 1.5 m downstream of the leading edge. At this location, the Reynolds number Re_L is 4×10^5, based on L and U_o.

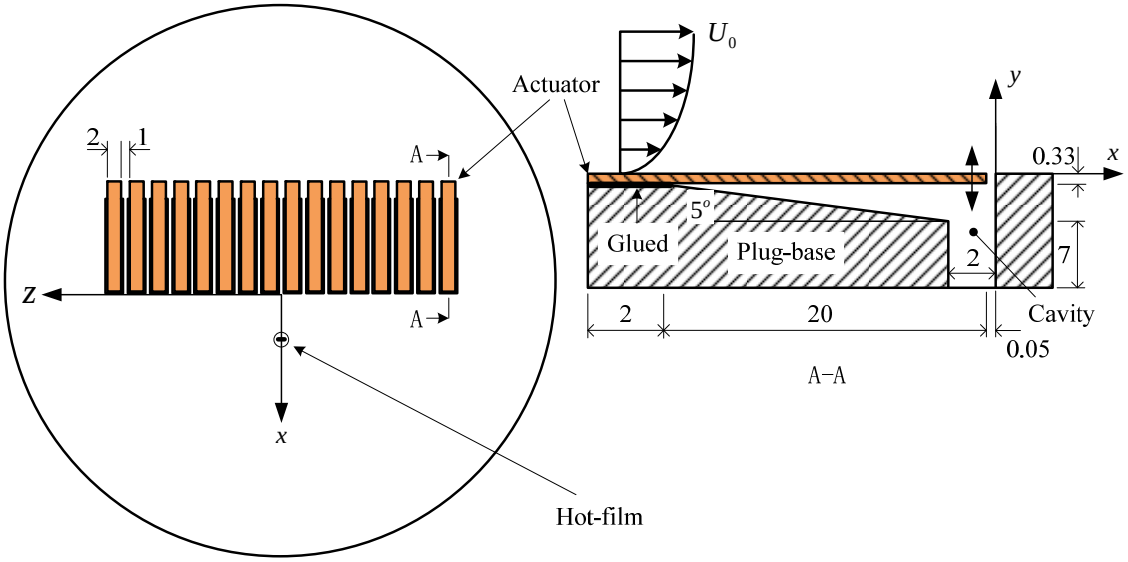

Fig. 1. The schematic of the spanwise-arranged actuator array (not in scale, units in mm)

Fig. 1 shows schematically the arrangement of actuators, each having a dimension of 22 mm × 2 mm × 0.33 mm (length × width × thickness). The actuators are cantilever-supported via gluing the inactive part (2 mm long) with the plug-base. The gap between the sides of the actuator and the wall edge around it is about 0.05 mm. There is a cavity under each actuator. The spacing between two adjacent actuators is 1 mm. As such, the entire actuator array spanned 45 mm in the transverse direction, covering 450 and 200 wall units along the spanwise and streamwise directions, respectively. The origin of the coordinate system is defined at the actuator tip, with x, y, and z along the streamwise, normal (to the wall) and spanwise (or transverse) directions, respectively.

The piezo-ceramic actuator used currently can work in a wide range of oscillation-frequencies (f), with the first resonance frequency around 400 Hz and the peak-to-peak amplitude (A) of the free tip about 0.5 mm, or 5 wall units. The dependence of A on f and voltage of the driving signal has to be calibrated individually for all 16 actuators, due to the fact that the actuators were assembled manually. Every actuator was driven by an individual voltage amplifier and guaranteed to have identical A by offsetting their driving voltages at each working frequency. Before being amplified, 16 channels of the driving signal were generated from a dSPACE control system (DS1006). The phase shift ($\phi_{i,i+1}$, i = 1, 2, …, 15) between two adjacent actuators was also set in the control system. In preliminary tests, three different $\phi_{i,i+1}$ (0^o, 24^o, or 180^o) and four different A, viz. 80 μm, 160 μm, 240 μm and 320 μm (or A^+ = 0.8, 1.6, 2.4 and 3.2), were examined, while the actuators oscillated at a frequency range of 50 Hz ~ 500 Hz (or an oscillation period T^+ from 3.5 to 35). For $\phi_{i,i+1} = 24^o$, the 16 actuators formed one wavelength (λ_w = 45 mm, or λ_w^+ = 450) of a traveling sinusoidal wave, corresponding to the phase velocity ($w_z = \lambda_w f$) from 2.25 m/s to 22.5 m/s (or w_z^+ = 12.78 ~ 127.8). For $\phi_{i,i+1} = 0^o$ and 180^o, the 16 actuators oscillated as a whole and in a caniniform, respectively.

A miniature single-wire probe (55P15, Dantec) was used to measure the streamwise velocity profile at the actuation location. The hot-wire probe has a Tungsten wire of 5 μm in diameter and about 2 mm in length, and was calibrated in the free stream with the aid of a Pitot tube. The probe was supported by a three dimensional traverse mechanism which has a high spatial resolution of 10 μm in y direction. A hot-film (55R45, Dantec) located at x = 5 mm or x^+ = 50 downstream of the actuator tip (Fig. 1) was used to determine the change in wall shear stress. Both the hotwire and the hot-film were connected to a Dantec Streamline anemometer and operated at a constant temperature mode, with an overheat ratio of 1.8. After being filtered at 1 kHz, the signals were sampled using a 16-bit A/D converter (NI PCI-6143) at 2.5 kHz. The recording of the hotwire signal was 40 seconds at each measuring point, while that of the hot-film signal was 200 seconds before and after actuation on.

The hot-film was calibrated *in situ* based on the mean of wall shear stress from the hotwire measurement. The mean velocity profile, close to the wall ($y^+ < 12$), was adopted to estimate the mean of wall shear stress at a free stream velocity ranging from 2 m/s to 6 m/s. It is pertinent to point out that there are unavoidable errors in the calibration due to the fact that the mean streamwise velocity, measured by the hotwire in the near-wall region, was influenced by the wall-normal fluctuations of the flow in the turbulent boundary layer. Nevertheless, the evaluation of the control performance should be insensitive to the errors since the change in wall shear stress in terms of percentage, instead of absolute values, is presently concerned. The measuring uncertainty of the hot-film was estimated to be within ±1%.

3. RESULTS AND DISCUSSION

In this section we will present and discuss preliminary results. The averaged change of wall shear stress is defined as $\Delta D^* = (D - D_o)/D_o$ (%), where D and D_o are time-averaged drags measured with and without control, respectively. Similarly, the averaged change of its root-mean-square (rms) value is defined as $\Delta rms^* = (rms - rms_o)/rms_o$ (%), in which rms and rms_o are the values measured with and without control, respectively.

Fig. 2 presents the measured mean streamwise velocity (U^+), its rms value (u_{rms}/u_τ), *Skewness* and

Kurtosis of the streamwise velocity in the boundary layer at the actuation location in the absence of control. The disturbance thickness (δ_{99}), displacement thickness (δ_1) and momentum thickness (θ) at the actuation location are estimated, based on U^+ (Fig. 2a), to be 54 mm, 7.9 mm and 5.8 mm, respectively, corresponding to a shape factor of H_{12} = 1.4. The friction velocity (u_τ) is estimated to be 0.176 m/s based on the mean velocity profile in the linear region. In Fig. 2a, the U^+ distribution agrees well with the universal law of a wall-bounded turbulent boundary layer. The constant in the log law is larger than 5.0, and this is because of the low Reynolds number effect. Moreover, the distribution of u_{rms}/u_τ has a maximum (around 3.0) at y^+ = 12 (Fig. 2b), where the *Skewness* runs through zero (Fig. 2c) and the *Kurtosis* arrives at its minimum (Fig. 2d) (Kim et al. 1987). These results indicate that the turbulent boundary layer is fully developed at the actuation location. Therefore, the averaged spanwise (λ_z) and longitudinal (λ_x) spacing between near-wall steaks, and the bursting frequency (f_B) may be estimated to be 10 mm, 100 mm, and 7 Hz, respectively, provided that the present flow is a canonical turbulent boundary layer (Kline et al. 1967, Blackwelder & Eckelmann 1977).

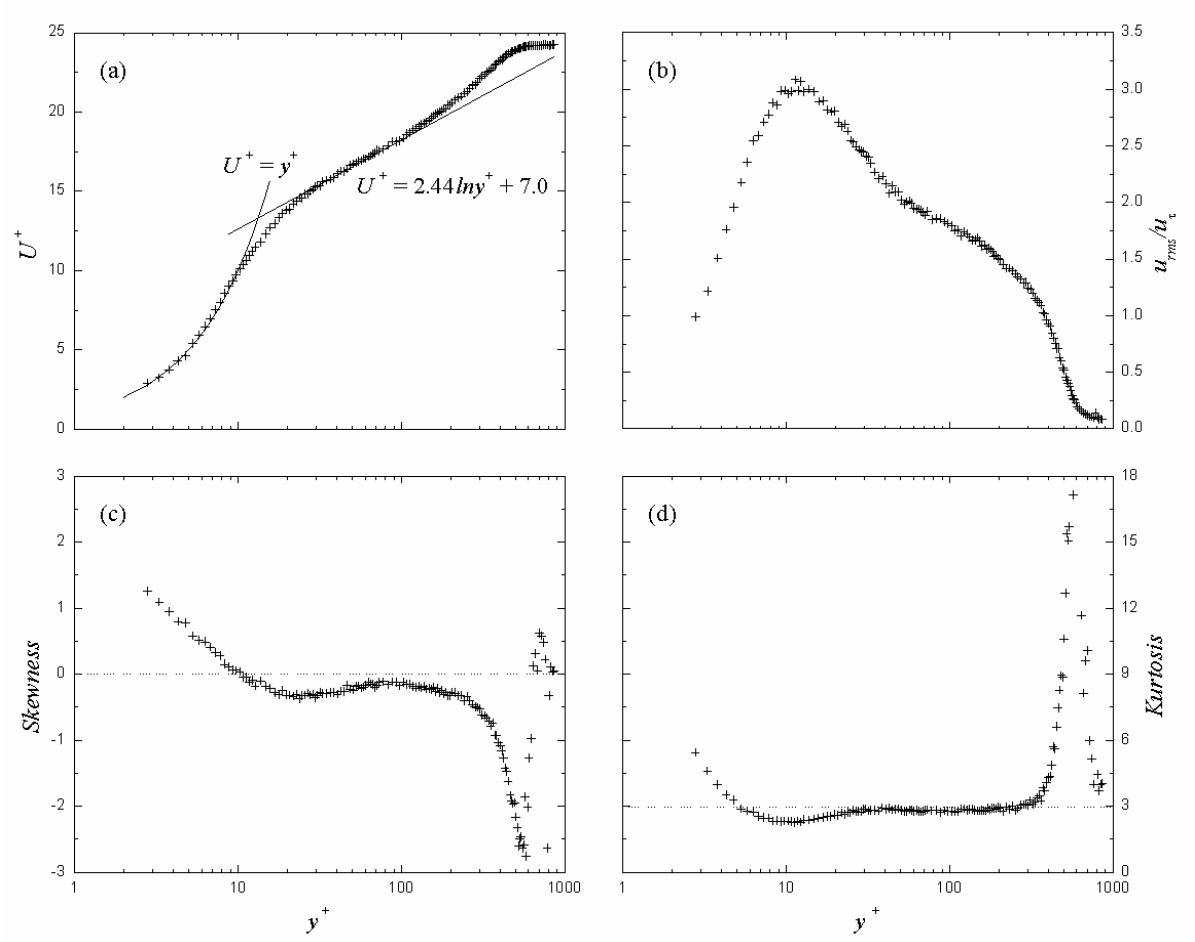

Fig. 2. The distributions of (a) U^+, (b) u_{rms}/u_τ, (c) *Skewness* and (d) *Kurtosis* with respect to the normal distance (y^+)

In order to disturb the coherent structures in a turbulent boundary layer, the physical size of an actuator is required to be in the order of 20 wall units and 200 wall units in the spanwise and streamwise directions, respectively, and its excitation frequency has to be at least 5 times of the bursting frequency (f_B) (Jacobson & Reynolds 1998). The actuators used currently satisfy these requirements. The width of the

actuator is only $0.2\lambda_z$, halving that used by Segawa et al. (2002). The streamwise extension of the cantilever-supported actuator is 200 wall units. As such, the entire array of 16 actuators covers a perturbation area of 4000, normalized by wall variables. The actuator worked at an oscillation-frequency (f^+) range from 0.0285 to 0.285, exceeding 5 times the natural bursting frequency ($f_B^+ \approx 0.004$) of the near-wall events.

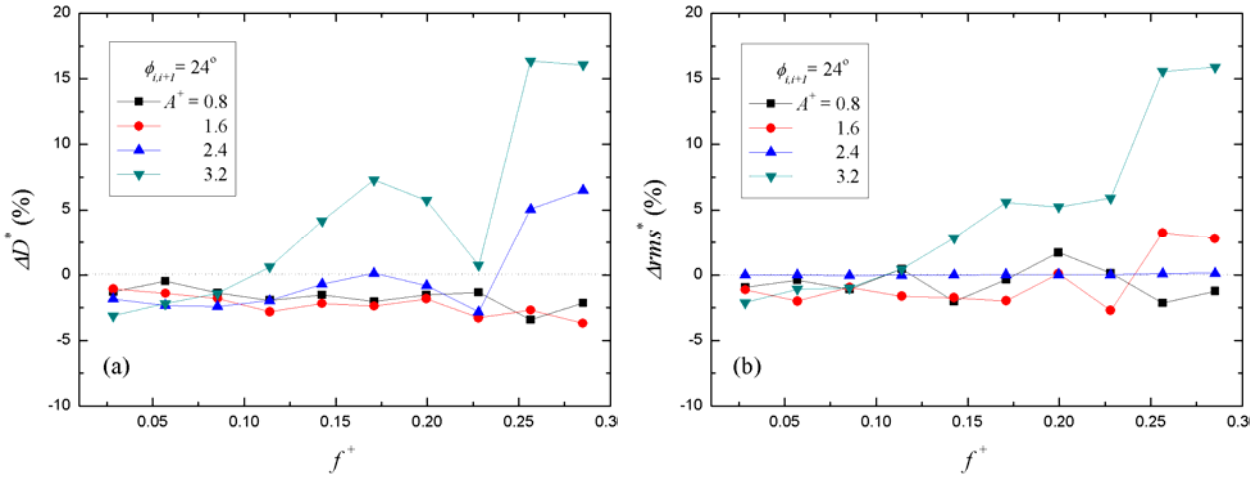

Fig. 3. The dependence of (a) ΔD^* and (b) Δrms^* on f^+ for $\phi_{i,i+1}$ = 24°

Jimémez & Pinelli's (1999) numerical experiment revealed that an autonomous cycle, which sustained the near-wall turbulence, existed between y^+ = 20 and 60, suggesting that acting directly on the near-wall streaks was an alternative strategy to control wall-bounded turbulence. In the current study, given $\phi_{i,i+1}$ = 24°, the 16 actuators formed one discrete sinusoidal wave travelling in the spanwise direction. It is expected that this transverse wave could suppress the activities of turbulence production by intervening the auto-sustainable coherent streaks in the near-wall region and thus reduce the wall shear stress. These discrete actuators oscillating in the wall-normal direction may also interact directly with the coherent structures. Fig. 3a shows the dependence of ΔD^* (%) on f^+ for four different A^+. It can be seen that ΔD^* is appreciable for the whole range of f^+ when A^+ is relatively small, i.e. A^+ = 0.8 and 1.6. Furthermore, ΔD^* tends to become larger with increasing f^+. In other words, the higher does the sinusoidal wave travel, the higher ΔD^* is obtained for these two smaller A^+. As A^+ increases to 2.4, drag increase is observed at $f^+ > 0.228$. For the largest A^+ = 3.2, only can drag reduction be obtained at $f^+ < 0.114$; in contrary, more than 15% drag increase results at $f^+ \geqslant 0.2565$. The valley for A^+ = 2.4 and 3.2, witnessed at f^+ = 0.228, may result from the resonance of the actuators. As the actuator was operated at its resonance frequency (around 400 Hz), the phase-frequency relationship was not definitive. The results seem to be consistent with Du et al.'s (2002) suggestion that the drag reduction strongly depended on energy input (or disturbance strength) through actuation into the flow. Large drag reduction would be achieved only when energy input was close to a threshold; otherwise, the near-wall streaks were unaffected or drag increase was observed. Du & Karniadakis (2000) and Du et al. (2002) also found that the drag reduction was dependent on the penetration length of the spatial travelling wave. To obtain a reduction in drag, the penetration length must be confined in the viscous sub-layer and the largest reduction was achieved (more than 50%) for a penetration length comparable to the viscous thickness. The amplitude of an actuator is linked to the penetration length, but its perturbation into the flow is larger than the stroke of the actuator because of the wall-normal oscillation. This may explain to some extent why drag increase was observed in a wide oscillation-frequency range ($f^+ \geqslant 0.114$), even though the largest A^+ = 3.2 is smaller than the viscous thickness.

The dependence of Δrms^* (%) on f^+ is shown in Fig. 3b, in which the Δrms^* is about zero for A^+ = 0.8,

1.6 and 2.4. Apparently, the *rms* value of wall shear stress was little affected by the sinusoidal wave when the amplitude was small ($A^+ \leqslant 2.4$). At A^+ =3.2, however, Δrms^* rises rapidly once f^+ exceeds 0.114, reaching more than 15% at $f^+ > 0.2565$.

As $\phi_{i,i+1} = 0^o$, the entire array of actuators oscillated in phase, resembling a waveform with 'infinite' wavelength. The dependence of ΔD^* and Δrms^* on f^+ is shown in Fig. 4a and Fig. 4b, respectively. In this case, the maximum of drag reduction (about 4.5%) is observed at $f^+ = 0.0855$ for $A^+ = 1.6$. On the other hand, the drag increase of near 20% was observed at $f^+ > 0.2565$ for the largest $A^+ = 3.2$.

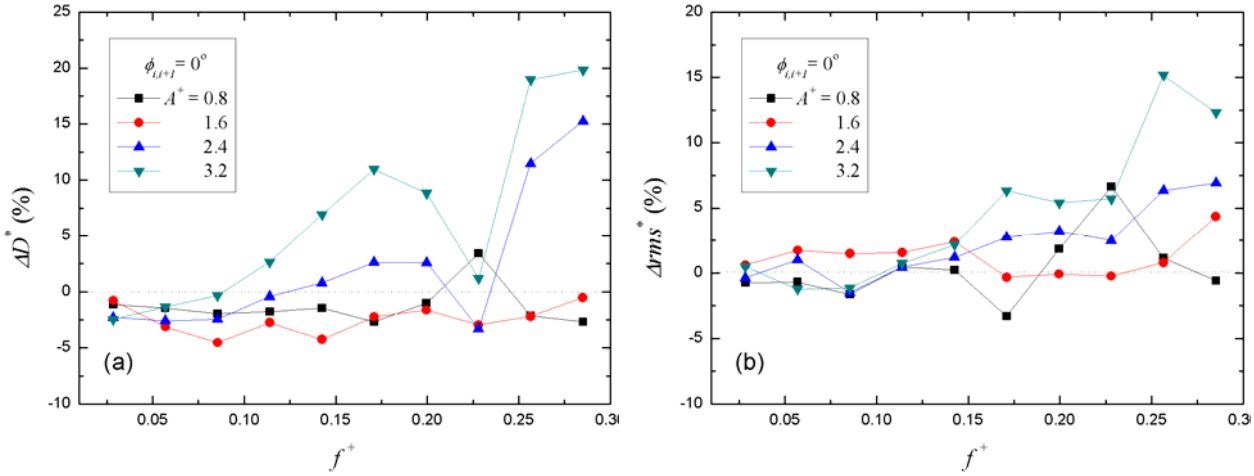

Fig. 4. The dependence of (a) ΔD^* and (b) Δrms^* on f^+ for $\phi_{i,i+1} = 0^o$

As $\phi_{i,i+1} = 180^o$, two adjacent actuators in the array oscillated in an anti-phase fashion, corresponding to no travelling wave. The dependence of ΔD^* and Δrms^* on f^+ is shown in Fig. 5a and Fig. 5b, respectively. In this case, no profound drag increase was observed except at $f^+ = 0.228$, at which the actuators worked resonantly. The largest drag reduction (about 5%) was obtained for $A^+ = 2.4$ at $f^+ = 0.285$. As a matter of fact, the drag reduction increases considerably from $f^+ = 0.2565$ to 0.285, irrespective of the value of A^+. It is highly likely that a higher f^+ may lead to a considerably increased drag reduction, which will be hopefully confirmed in our on-going experiments. For the *rms* value, its maximum increasing for $A^+ = 3.2$ at $f^+ = 0.285$ was about 8%, much lower than that in other two cases.

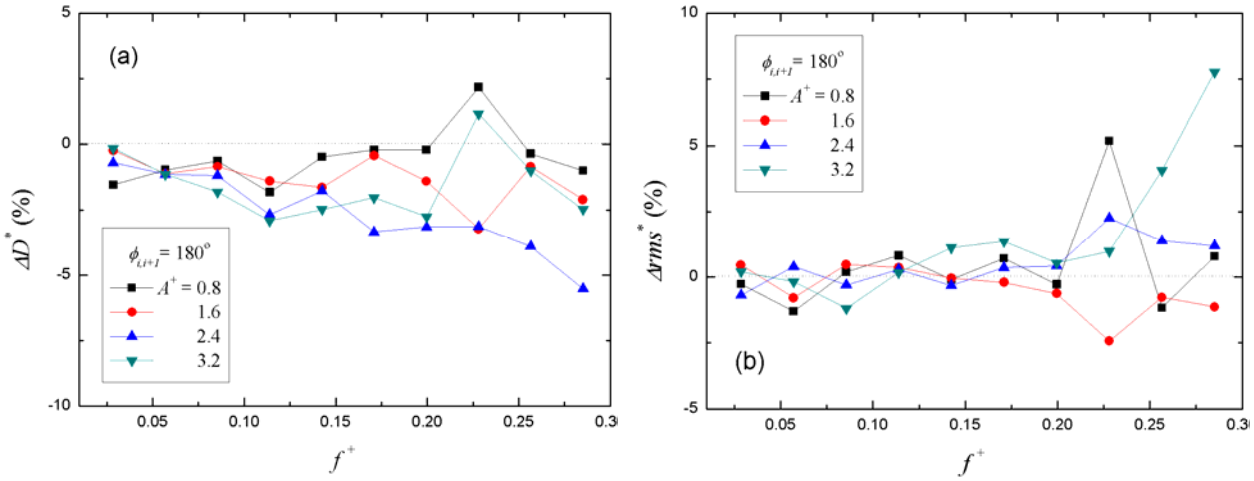

Fig. 5. The dependence of (a) ΔD^* and (b) Δrms^* on f^+ for $\phi_{i,i+1} = 180^o$

4. CONCLUSION

Drag reduction in a turbulent boundary layer based on a spanwise array of actuators was experimentally investigated. Three waveforms with four different amplitudes were formed by these actuators working in a wide range of the oscillation frequencies. Though preliminary, experimental results show a drag reduction of up to 5% when the wave was in a caniniform ($A^+ = 2.4$) and worked at $f^+ = 0.285$. Investigations are on-going to use different control strategies such as different actuation signals, spanwise travelling wavelengths and speeds, etc. in order to achieve better results in terms of drag reduction.

ACKNOWLEDGMENTS

YZ wishes to acknowledge support given to him by the Research Grants Council of the Government of the HKSAR through Grant PolyU 5334/06E.

REFERENCES

Blackwelder RF and Eckelmann H (1977) The spanwise structure of the bursting phenomenon. In *Structure and Mechanisms of Turbulence* I, edited by Fiedler H, Berlin, Springer

Choi K-S, DeBisschop J-R and Clayton BR (1998) Turbulent boundary-layer control by means of spanwise-wall oscillation. *AIAA J.* **36(7)**:1157-1163

Choi H, Moin P and Kim J (1994) Active turbulence control for drag reduction in wall-bounded flows. *J. Fluid Mech.* **262**:75-110

Du Y and Karniadakis GE (2000) Suppressing wall turbulence by means of a transverse travelling wave. *Science* **288**:1230-1234

Du Y, Symeonidis V and Karniadakis GE (2002) Drag reduction in wall-bounded turbulence via a transverse travelling wave. *J. Fluid Mech*. **457**:1-34

Jacobson SA and Reynolds WC (1998) Active control of streamwise vortices and streaks in boundary layers. *J. Fluid Mech*. **360**: 179-211

Jimémez J and Pinelli A (1999) The autonomous cycle of near-wall turbulence. *J. Fluid Mech*. **389**: 335-359

Jung WJ, Mangiavacchi N and Akhavan R (1992) Suppression of turbulence in wall-bounded flows by high-frequency spanwise oscillations. *Phys. Fluids A* **4(8)**:1605-1607

Karniadakis GE and Choi K-S (2003) Mechanism on transverse motions in turbulent wall flows. *Annu. Rev. Fluid Mech*. **35**:45-62

Kim J, Moin P and Moser R (1987) Turbulence statistics in fully developed channel flow at low Reynolds number. *J. Fluid Mech.* **177**: 133-166

Kline SJ, Reynolds WC, Schraub FA, Runstadler PW (1967) The structure of turbulent boundary layers. *J. Fluid Mech.* **30 (4)**: 741-773

Kravchenko AG, Choi H and Moin P (1993) On the relation of near-wall streamwise vortices to wall skin friction in turbulent boundary layers. *Phys. Fluids A* **5(12)**:3307-3309

Quadrio M and Ricco P (2004) Critical assessment of turbulent drag reduction through spanwise wall oscillations. *J. Fluid Mech*. **521**:251-271

Segawa T, Kawaguchi Y, Kikushima Y, Yoshida H (2002) Active control of streak structures in wall turbulence using an actuator array producing inclined wavy disturbances. *J. Turbulence* **3**: 1-15